Na^+/H^+ Exchanger NHE3 Has 11 Membrane Spanning Domains and a Cleaved Signal Peptide: Topology Analysis Using In Vitro Transcription/Translation†

Mirza Zizak,‡,|| Megan E. Cavet,‡,|| Denis Bayle,§ Chung-Ming Tse,‡ Stefan Hallen,§ George Sachs,§ and Mark Donowitz*,‡

From the Departments of Medicine and Physiology, GI Unit, The Johns Hopkins University School of Medicine, Baltimore, Maryland 21205 and UCLA/Wadsworth Veterans Administration Hospital, Los Angeles, California 90073

Received April 17, 2000

ABSTRACT: The transmembrane topology of Na^+/H^+ exchanger NHE3 has been studied using in vitro transcription/translation of two types of fusion vectors designed to test membrane insertion properties of cDNA sequences encoding putative NHE3 membrane spanning domains (msds). These vectors encode N-terminal 101 (HKM0) or 139 (HKM1) amino acids of the H,K-ATPase α-subunit, a linker region and a reporter sequence containing five N-linked glycosylation consensus sites in the C-terminal 177 amino acids of the H,K-ATPase β-subunit. The glycosylation status of the reporter sequence was used as a marker for the analysis of signal anchor and stop transfer properties of each putative msd in both the HKM0 and the HKM1 vectors. The linker region of the vectors was replaced by sequences that contain putative msds of NHE3 individually or in pairs. In vitro transcription/translation was performed using [^{35}S]methionine in a reticulocyte lysate system ± microsomes, and the translation products were identified by autoradiography following separation using SDS−PAGE. We propose a revised NHE3 topology model, which contains a cleaved signal peptide followed by 11 msds, including extracellular orientation of the N-terminus and intracellular orientation of the C-terminus. The presence of a cleavable signal peptide in NHE3 was demonstrated by its cleavage from NHE3 during translational processing of full-length and truncated NHE3 in the presence of microsomes. Of 11 putative msds, six (msds 1, 2, 4, 7, 10, and 11) acted as both signal anchor and stop transfer sequences, while five (msds 3, 5, 6, 8, and 9) had signal anchor activities when tested alone. Of the latter, 3, 5, 6, and 9 were shown to act as stop transfer sequences after C-terminal extension. The actual membrane orientation of each sequential transmembrane segment of NHE3 was deduced from the membrane location of the N- and C-termini of NHE3. The regions between putative msds 8 and 9 and between msds 10 and 11, which correspond to the fourth and fifth extracellular loops, did not act as msds when tested alone. However, the extension of the fifth extracellular loop with adjacent putative msds showed some membrane-associated properties suggesting that the fifth extracellular loop might be acting as a "P-loop"-like structure.

Na^+/H^+ exchangers (NHEs)[1] are polytopic integral membrane proteins that mediate the electroneutral exchange of intracellular H^+ for extracellular Na^+ across plasma membranes. Molecular cloning studies have revealed six distinct mammalian NHEs isoforms (NHE1−6) (*1*). Overall, NHE1−5 share ∼30−60% sequence homology with a predicted molecular mass between ∼81−93 kDa. To date, the actual topology of the NHE gene family has not been systematically studied. Immunocytochemical studies and hydropathy analyses predict that all cloned NHEs have two distinct domains: ∼450−500 a.a.-long transmembrane hydrophobic N-terminus and ∼300 a.a.-long relatively hydrophilic C-terminus. While the cytoplasmic domain is very variable sharing from ∼25−30% identity among isoforms, the N-terminal transmembrane domains share a high amino acid sequence homology (∼60%) among the various isoforms. Studies with deletion mutants and chimeric NHEs revealed that the NHE C-terminal domain is required for short-term regulatory responses and is intracellular (*2*−*4*). The intracellular localization of the NHE C-terminus was identified based on immunocytochemical studies in which antibodies raised to the C-terminal 85 a.a. of NHE3 (*5*) and 157 a.a. of NHE1 (*6*) could bind to their epitopes only after cell permeabilization. Furthermore, FGF stimulated NHE3 truncated to a.a. 509 but not to a.a. 475, showing that this portion of NHE3 immediately C-terminal to a.a. 475 was necessary for

† This work was partially supported by the National Institutes of Health (NIH) Grants RO1 DK26523, PO1 DK44484, and RO1 DK51116, Fogarty International Center NIH TW05234, Wellcome International Travelling Fellowship, and The Hopkins Center for Epithelial Disorders.

* To whom correspondence should be addressed: Mark Donowitz, MD, GI Division, Department of Medicine, The Johns Hopkins University School of Medicine, 925 Ross Research Bldg., 720 Rutland Ave., Baltimore, MD 21205-2195. Telephone: 410-955-9675; fax: 410-955-9677; e-mail: mdonowit@welch.jhu.edu.

‡The Johns Hopkins University School of Medicine.

§UCLA/Wadsworth Veterans Administration Hospital.

|| These authors contributed equally to this work.

[1] Abbreviations: NHE, Na^+/H^+ exchanger; msd, membrane spanning domain; SP, signal peptide; PNGase F, peptide:*N*-glycosidase; el, extracellular loop; a.a., amino acid; SA, signal anchor sequence; ST, stop transfer sequence.

10.1021/bi000870t CCC: $19.00
Published on Web 06/13/2000

stimulation and was intracellular (*7*). In addition, the identification of calmodulin binding sites within the C-termini of NHE1 (8), NHE2 (*9*), and NHE3 (*10*) support their intracellular localization. However, there is conflicting evidence on this point. A recent study using monoclonal antibodies raised to the C-terminal 131 a.a. of NHE3, but for which the epitopes have not been identified, showed that these antibodies can bind to their epitopes without cell permeabilization when added externally to intact cells or right-side-out vesicles (*11*).

The hydropathy profiles of NHEs predict the presence of 10−12 hydrophobic segments that form membrane-spanning domains. It has been demonstrated that N-terminal transport domains of the NHEs preserve their transport function despite complete removal of their C-termini. These studies revealed that the isolated N-termini (in NHE3 a.a. 1−475) retain the ability to insert into the membrane, dimerize, and perform amiloride-sensitive Na^+/H^+ exchange activity, although at a much lower rate than the wild-type NHEs (*12*). These truncated NHEs can be activated by intracellular H^+, also indicating the presence of an H^+ modifier site within their N-termini (*3*).

Additional NHE topological data have been obtained from glycosylation studies and studies with sequence-specific antibodies, immunofluorescence, and electron microscopy. Glycosylation studies have shown that NHE1 is N- and O-glycosylated on the first extracellular loop, indicating its extracellular localization (*13*). Similarly, NHE2 is O- but not N-glycosylated on this loop (*14*). This observation was complemented by recent immunocytochemical studies in which the visualization of antibodies, raised to HA epitopes inserted into the region comprising a.a. 38−41 of NHE3, was obtained without cell permeabilization (*15*). Interestingly, a single N-glycosylation consensus site at residue N^{325} in NHE3 and a corresponding region in the other NHE isoforms does not appear to be glycosylated in the intact protein (*14*). Furthermore, studies on NHE1 in which antibodies failed to visualize an epitope fused to the extreme N-terminus (*12*), suggested the presence of a cleavable signal peptide in the N-termini of NHEs that is cleaved off during protein processing. Of note is the high divergence in this part of the N-termini of NHEs as compared with high sequence homology in the rest of the NHE N-termini.

In this report, we systematically test a putative model of NHE3 topology by using in vitro transcription/translation analysis. The aims were to (i) test the current NHE3 topology model, (ii) determine whether NHE3 contains a cleavable signal peptide, and (iii) determine the membrane orientation of putative msds.

EXPERIMENTAL PROCEDURES

Vector Construction and Strategy. To analyze the topogenic properties of putative transmembrane segments of NHE3, two different vectors, HKM0 and HKM1, were used for in vitro transcription/translation. These vectors, which were designed for detection of msds of the gastric H,K-ATPase, were previously constructed by modification of the α- and β-subunits of the gastric H,K-ATPase (*16*). Both expression vectors were cloned into the plasmid pGEM7zf+-(Δ*Hin*dIII), in which the *Hin*dIII site in the cloning region was removed.

These two fusion vectors encode amino-terminal 101 (HKM0 vector) or 139 (HKM1 vector) amino acids of the H,K-ATPase α-subunit, a linker region and the reporter sequence containing the carboxyl-terminal 177 amino acids of the H,K-ATPase β-subunit. Eight positively charged amino acids retain the amino-termini of the HKM0 and HKM1 fusion proteins on the cytoplasmic side of the microsomal membranes (*17*). The linker region of the vectors was replaced by sequences that contain putative msds of NHE3 individually or in pairs. The glycosylation status of the reporter sequence containing five N-linked (NXT/S) glycosylation consensus sites was used as a marker for the analysis of signal anchor (SA) and stop transfer (ST) properties of each putative msd. The glycosylation of those N-linked consensus sites represent the translocation of the reporter sequences of these fusion vectors into the lumen of microsomes and was verified by a mobility shift on SDS−PAGE observed after translation of the constructs in the absence and presence of microsomes.

The difference between these two vectors was used to determine the membrane properties of putative msds. The native HKM0 vector does not contain a transmembrane segment, whereas the HKM1 vector contains the transmembrane segment that originates from the first msd of H,K-ATPase. Therefore, the native HKM0 vector is not glycosylated, while the native HKM1 vector is glycosylated when translated in the presence of microsomes. The presence of a msd in the linker region translocates the HKM0 reporter sequence into the lumen of the microsomes and, subsequently, causes the glycosylation of the fusion protein. Such a sequence is characterized as an SA sequence. Likewise, an msd that translocates the HKM1 reporter sequence out of the lumen of microsomes and, subsequently, prevents glycosylation of HKM1 is characterized as an ST sequence.

Polymerase Chain Reaction and Ligation. Amplification of cDNA encoding putative msds of NHE3 was carried out in a 100-μL reaction containing 0.3 μM concentration of each primer (the sense primer contained a *Bgl*II, and the antisense primer contained a *Hin*dIII restriction site), 1 ng of the template, 200 μM deoxynucleotides (Pharmacia Biotech Inc.) in a buffer supplied by the manufacturer, and 2 units of *Taq* polymerase (BRL). The PCR products were digested with *Bgl*II and *Hin*dIII, and DNA fragments were separated on 2% agarose gels for purification using a PCR purification kit (Qiagen). The purified PCR fragments were ligated using T4 DNA ligase into the *Bgl*II and *Hin*dIII sites of the HKM0 and HKM1 vectors. Ligation and transformation of plasmids were performed according to standard protocols. The expression plasmids containing the selected sequences were transformed in One Shot cells (InVitrogen) and purified using anion exchange chromatography (Qiagen). The DNA sequences inserted into the HKM0 and HKM1 expression vectors were verified by dideoxy sequencing.

In Vitro Transcription/Translation Reactions. Membrane insertion properties of all the selected sequences were tested in both the HKM0 and HKM1 vectors by in vitro transcription/translation reactions using the TNT-coupled rabbit reticulocyte lysate system (Promega). These reactions were performed in the presence of [^{35}S]methionine (Amersham) according to the manufacturer's instructions and carried out at 30 °C for 2 h in the absence or presence of canine pancreatic microsomal membranes (Promega). Reaction

mixtures in the absence of the microsomal membranes constituted the negative controls. Each transcription/translation reaction was performed at least three times.

Signal Peptide Analysis. The ability of microsomal vesicles to cleave a signal peptide from the associated protein was used to test for the presence of a cleaved signal peptide in NHE3. Full-length NHE3 cDNA was first cloned into the pBS expression vector, which contains the T7 RNA polymerase promoter. Truncations of NHE3 at a.a. 124 (sense primer AGAGGCGATGTCAGGGCGCGG; antisense primer GTAGCCGGCGTCCAGCACGATGG) and a.a. 284 (sense primer AGAGGCGATGTCAGGGCGCGG; antisense primer CTCGATGACGCGCACGTGCTTGG) were synthesized by PCR. The constructs were cloned into pCR2.1, containing the T7 RNA polymerase promoter. Transcription/translation reaction was carried out as described above. The processing efficiency of the microsomal membranes was tested with the positive control mRNA supplied with the microsomal membranes.

Alkaline Extraction of Microsomal Membranes. The presence of the translated fusion proteins in microsomal membranes was tested by alkaline extraction. The microsomal pellet was extracted with sodium carbonate (7.5 μL of the reaction mix was diluted with 150 μL of 0.1 M Na_2CO_3, pH 11) and left at 4 °C for 30 min. The membranes were pelleted by centrifugation in a Beckman ultracentrifuge (TL-100) at 100000*g* for 30 min, and the pellet was resuspended in 250 mM sucrose and 50 mM Tris-HCl, pH 7.4. The samples were solubilized in sample buffer (110 mM Tris HCl, 1.8% SDS, 0.16% EDTA 3Na, 10% glycerol, 2% β-mercaptoethanol, and bromophenol blue). As a control for adhesion rather then insertion of the translated products, microsomal membranes were added after translation and extracted as described above.

PNGase F Digestion. Verification of glycosylation of the fusion proteins in the membrane of microsomes was tested by incubation with PNGase F (1000 units) (New England Biolabs) at 37 °C for 60 min, according to the manufacturer's protocol.

SDS−PAGE and Autoradiography. The reaction mixtures were separated electrophoretically on 10% SDS−polyacrylamide gels. Translation products synthesized in the absence or presence of microsomal membranes were run on lanes next to each other. The reaction volume loaded onto the gel in the presence of microsomes was double that in the absence of microsomes, due to decreased translation efficiency when the microsomal membranes were present. After electrophoresis, gels were fixed for 20 min in 50% methanol and 10% acetic acid buffer, dried, and subjected to autoradiography overnight at room temperature. The gels with the samples subjected to alkaline extraction were stained with 0.1% Coomassie Brilliant Blue in 50% methanol and 10% acetic acid buffer and washed in the same buffer without dye to assess the amount of translated product measured after alkaline extraction.

Predictions of Transmembrane Sequences. Seven separate computer algorithms were used to predict the number and the boundaries of putative msds of NHE3. The putative msds were predicted from 18 to 22 amino acid-wide sliding window averages of the amino acid hydrophobicities. Some of these algorithms predict putative msds based only on the prediction of transmembrane α-helices, while others are based empirically and thermodynamically on the hydrophobic partitioning of amino acid residues (*18*−*22*). Figure 1 illustrates an example of the NHE3 amino-domain sequence hydropathy profile (using the Kyte−Doolittle method) with 13 predicted transmembrane segments indicated (including SP and el5). El5 was predicted to be an msd by 5 of 7 algorithms. The initial prediction of putative msds of NHE3 relied on the Predict Protein (PredictP) neural network algorithm, which predicts transmembrane helices in integral membrane proteins by multiple sequence alignments. This algorithm was chosen as the basic algorithm due to its documented very high accuracy in prediction of transmembrane segments of multiple proteins with experimentally determined locations of transmembrane helices (*19*, *23*). Six additional computer algorithms were used to further predict the number and the boundaries of putative msds of NHE3. As shown in Table 1, these seven algorithms predicted that NHE3 had between 10 and 14 putative msds. Seven putative msds in our final model (Figure 2) were predicted by all hydropathy algorithms (msds 1, 2, 4, 7, 8, 10, and 11); three putative msds were predicted by six (signal peptide, msds 5 and 9) and three msds were predicted by five algorithms (msds 3, 6, and el5). Those putative msds that were predicted by at least five of seven algorithms were tested by the in vitro transcription/translation system for their SA and ST properties. In addition, following the positive charge rule (*24*), the boundaries of sequences predicted to contain putative msds were designed to include contiguous positive amino acid residues whenever possible (Table 2).

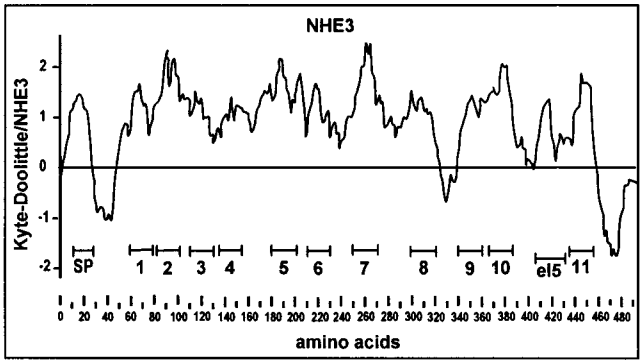

FIGURE 1: Hydropathy plot of the amino-terminal half of the NHE3 sequence. The hydropathic profile of the amino-terminal domain of the NHE3 sequence is calculated by the method of Kyte−Doolittle using a 22-amino acid window. Lanes below the plot show putative transmembrane segments, which are indicated from 1 to 11, SP and el5.

RESULTS

To allow interpretation of the experimental results, a working model of the topology of NHE3 is shown in Figure 2, which is supported by the results from these current studies. This model contains 11 putative msds with an N-terminal signal sequence, which is cleaved from the rest of the NHE3 protein, an extracellularly located N-terminus, and an intracellular C-terminus (*1*, *5*, *25*). The msd boundaries shown were determined primarily by the Predict Protein algorithm, which has the ability to assess the extent to which residues embedded in a protein structure are accessible to solvent. This approach allowed us to generate testable constructs of each putative msd of NHE3.

HKM1 and HKM0 Fusion Proteins. In vitro transcription/translation of the HKM0 fusion protein alone showed no shift

Table 1: Hydropathy Predictions of Transmembrane Sequences of the Na^+/H^+ Exchanger NHE3[a]

put msd	method of Kyte−Doolittle	predict from MEMSAT	method of Eisenberg	method of Rao and Argos	predict from HMMTOP	predict from TMpred	predict from PredictP	designed constructs (NHE3 a.a.)	tested msd
1**	12−27	5−25	6−26	5−24	5−24	8−25		1−124; 1−284	
2*	60−79	55−71	54−74	56−73	56−75	55−74	56−73	55−78	1
3*	82−101	85−101	80−100	83−127	85−109	85−102	79−96	76−99	2
4***	111−130	108−124	104−124			104−130	109−127	110−133	3
5*	135−154	134−152	134−154	134−199	141−165	134−154	142−161	138−165	4
6			158−178						
7**	181−200	175−199	180−200		175−199	175−198	178−195	174−199	5
8***	210−229	207−229	207−227		217−236	207−233		207−230	6
9*	250−269	250−274	250−270	246−275	250−274	256−275	249−270	248−276	7
10*	299−319	283−299	283−303	287−318	288−312	303−322	288−312	288−312	8
11		307−321							
12**	340−359	340−359	338−358	340−359	344−363		345−362	339−365	9
13*	367−385	367−387	360−380	361−392	373−392	360−380	368−388	369−395	10
14***		406−425	405−425	410−425	406−425	410−427		406−431	el5
15*	436−455	435−455	435−455	435−455	435−455	435−453	436−453	435−456	11

[a] Segments of NHE3 are listed that are predicted to be membrane-spanning domains by any of the seven algorithms used to analyze the membrane topology of NHE3. These algorithms predict that NHE3 has 10 [Rao & Argos (*18*), PredictP (*19*)], 12 [Kyte & Doolittle (*20*), HMMTOP (*34*), Tmpred (*35*)] or 14 putative msds [Eisenberg (*21*), MEMSAT (*22*)]. Putative msds predicted by all programs are marked with (*). Msds predicted by six out of the seven programs are marked with (**), and those predicted by five algorithms are marked with (***). Numbering of NHE3 amino acids starts at the translation start site. Those putative msds that were predicted by at least five algorithms were tested for membrane-insertion capacity. Last column on right refers to final model in Figure 2.

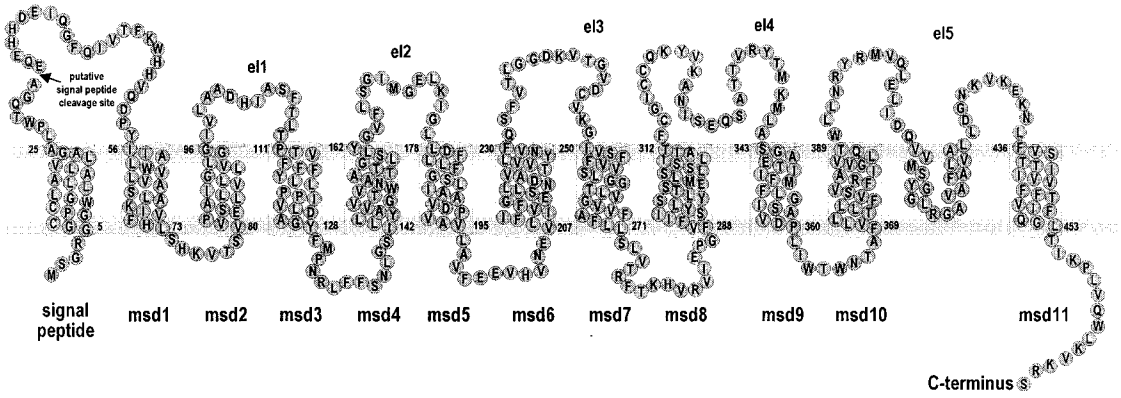

FIGURE 2: Primary amino acid sequence and predicted secondary structure model of the N-terminus of rabbit NHE3. Figure shows the transmembrane portion of the proposed NHE3 model based on the predictions deduced from multiple computer algorithm analyses of the NHE3 primary sequence and the results obtained by the in vitro transcription/translation technique. The N-terminus is followed by a large hydrophilic C-terminal portion that is located intracellularly and is not shown here. The first transmembrane segment on the N-terminus of NHE3 is cleaved as a signal peptide during protein processing. The amino acid sequence deduced from the nucleotide sequence of rabbit NHE3 cDNA is presented by single-letter code. Each transmembrane segment is numbered (msd 1−11), while the numbers in each msd represents the putative borders of the predicted transmembrane segment. El stands for extracellular loop.

in apparent molecular mass in the presence of microsomal membranes (Figure 3, lanes 1 and 2). As reported, HKM0 does not contain a sequence with msd properties and was not membrane-inserted during protein synthesis (*26*). In contrast, a 12.5-kDa shift in molecular weight in the presence of microsomes was obtained with HKM1 (Figure 3, lanes 3 and 4), which corresponds to five glycosylation consensus sites in the reporter sequence, as reported (*26*). As is shown in Figure 3, lane 5, the size shift observed after translation of HKM1 in the presence of microsomes disappeared after treatment with PNGase F, demonstrating that this was a glycosylated product.

NHE3 Contains a Cleaved Signal Peptide. The presence of a signal peptide in NHE3 and its putative cleavage site at a.a. 30 of NHE3 were predicted by the SignalP algorithm (*27*). This prediction was tested by using the ability of microsomal signal peptidases to cleave signal peptides. In vitro transcription/translation of full-length NHE3 was performed in the absence and presence of microsomes. In the absence of microsomes, a protein product of ~90 kDa was obtained, and in the presence of microsomes a decrease in molecular weight was observed (Figure 4A). Identification of the NHE3 protein after translation was performed using a polyclonal anti-NHE3 antibody (Ab 1381), which recognizes a C-terminal epitope (*5*) (data not shown). This shows that the decrease in size comes from the N- rather than the C-terminus. These data were supported by translation of truncations of NHE3 with and without microsomes. Both NHE3 truncated at a.a. 124 and a.a. 284 showed a partial shift of approximately 3 kDa in the presence of microsomes (Figure 4B). Thus, these data suggest the cleavage of the N-terminus and support the presence of a cleavable signal peptide in NHE3, as schematically illustrated in Figure 4C.

Analysis of Predicted Msds by In Vitro Transcription/Translation. Putative msd sequences of NHE3, individually or in pairs, were introduced into the HKMO and HKM1 vectors to analyze the topologic properties of predicted msds of NHE3. The ability of msds to insert in the membrane was determined by the presence or absence of glycosylation. Each glycosylated product was treated with PNGase F to

Table 2: Putative Membrane-Spanning Domains of NHE3 and Summary of Transcription/Translation Results[a]

tested msd	sequence	NHE3 a.a.	glycosylation in HKM0	glycosylation in HKM1	SA/ST
1	YIIALWVLVASLAKIVFHLSHKVT	55−78	+	−	SA/ST
2	KVTSVVPESALLIVLGLVLGGIV	76−99	+	−	SA/ST
3	TPTVFFFYLLPPIVLDAGYFMPNR	110−133	+	+	SA/−
4	NLGSILLYAVVGTVWNAATTGLSLYGVF	138−165	+	−	SA/ST
5	KIGLLDFLLFGSLIAAVDPVAVLAVF	174−199	+	+	SA/−
6	VLFIIVFGESLLNDAVTVVLYNVF	207−230	+	+	SA/−
7	KGIVSFFVVSLGGTLVGVVFAFLLSLVTR	248−276	+	−	SA/ST
8	FVFIISYLSYLTSEMLSLSSILAIT	288−312	+	+	SA/−
9	KMLASGAETIIFMFLGISAVDPLIWTW	339−365	+	+	SA/−
10	FVLLTLLFVSVFRAIGVVLQTWLLNRY	369−395	+	−	SA/ST
el5	VVMSYGGLRGAVAFALVALLDGNKVK	406−431	−	+	−/−
11	LFVSTTIIVVFFTVIFQGLTIK	435−456	+	−	SA/ST
1−2	YIIAL... ...VLGGIV	55−99	nd	+	
3−4	TPTVFF.....SLYGVF	110−165	nd	+	
4−5	NLGSIL... ...AVLAVF	138−199	−	+	
5−6	KIGLLD... ...VLYNVF	174−230	nd	+	
6−7	VLFIIV... ...LSLVTR	207−276	−	+	
9−10	KMLAS... ...WLLNRY	339−395	−	+	
10-el5	FVLLTL... ...DGNKVK	369−431	+	+	
el5−11	VVMSYG.... ...QGLTIK	406−456	+	+	
10−11	FVLLTL... ...QGLTIK	369−456	+	+	
el4	KYVKA... ...RYTMK	320−339	−	+	−/−

[a] Listed below are the segments of NHE3 that are predicted to be putative msds and tested for their membrane insertion capacity. In the first column, tested putative msds are indicated by their final msd number in the proposed NHE3 model (Figure 2). SP stands for signal peptide, and el4 and el5 stand for putative extracellular loops 4 and 5. Sequence indicates the amino acid sequence of NHE3 inserted into HKM0 and/or HKM1 vectors. In the constructs consisting of two putative msds, the loops between these segments were contained in the inserted sequence. Where the sequences were too long to list, the N- and C-termini of the sequences are listed connected with dots. In the glycosylation column is shown whether the insert allows the glycosylation of the HKM0 and HKM1 constructs: (+) stands for the presence of glycosylation, (−) stands for the absence of glycosylation, and nd stands for not determined. The SA/ST column indicates the ability of the putative msds to act as a signal anchor (SA) or as a stop transfer (ST); (−) stands for the inability of the putative msds to act as SA or ST.

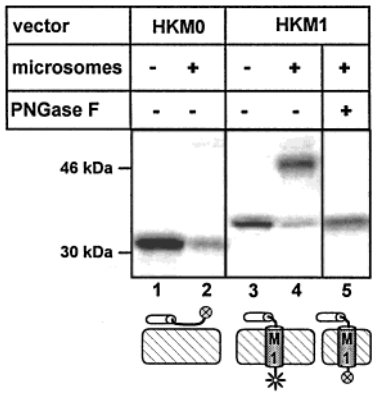

FIGURE 3: In vitro transcription/translation of the HKM0 and HKM1 vectors without inserts and effect of PNGase F digestion of HKM1 vector translated in the presence of microsomal membranes. SDS−PAGE analysis of the translated fusion proteins obtained by in vitro transcription/translation of the HKM0 (lanes 1 and 2) and HKM1 (lanes 3 and 4) constructs, in the absence (−) and presence (+) of microsomes. [^{35}S]Met-labeled translated products were visualized by autoradiography. The HKM1 construct translated in the presence of microsomes was incubated with PNGase F. The deglycosylated product was the same size as the HKM1 protein translated in the absence of microsomes (lane 5). Asterisk (*) represents glycosylation of the reporter sequence and (⊗) stands for the nonglycosylated reporter sequence.

confirm that the 12.5-kDa elevation of apparent molecular size found after translation in the presence of microsomes was due to the glycosylation. In addition, alkaline extractions of microsomal membranes containing translation products that were not glycosylated were performed to confirm that the translation products were present in the membrane. Examples of these procedures are shown in Figure 5.

Msd 1 (a.a. 55−78). Putative msd 1 inserted into the HKM0 vector promoted a 12.5-kDa increase in molecular size of the translated products in the presence of microsomes (Figure 5, lanes 1 and 2). This increase indicated glycosylation of the reporter sequence and characterizes msd1 as an SA sequence. Insertion of the same sequence into the HKM1 vector prevented the glycosylation of the reporter sequence in the presence of microsomes. This indicated the ability of msd1 to act as an ST sequence (Figure 5, lanes 3 and 4).

Msd 2 (a.a. 76−99). Putative msd 2 in the HKM0 vector caused a 12.5 kDa shift in molecular size of the translated protein in the presence of microsomes (Figure 5, lanes 5−6). PNGase F treatment confirmed that the increase in molecular size was due to glycosylation (Figure 5, lane 7). Insertion of the same sequence into the HKM1 vector prevented the glycosylation of the reporter sequence in the presence of microsomal membranes (Figure 5, lanes 8−9). The presence of the translated products in microsomal membranes was confirmed by alkaline extraction (Figure 5, lane 10). Therefore, putative msd 2 can act as both an efficient SA and ST sequence.

Msd 1 and 2 (a.a. 55−99). When the HKM1 vector containing putative msds 1 and 2 was translated in the presence of microsomes, a glycosylated protein was obtained (Figure 5, lanes 11 and 12). This indicated the presence of a pair of transmembrane segments in the inserted sequence, in which putative msd 1 acts as an ST and putative msd 2 as an SA sequence. The ST property of msd 1 in native NHE3 was expected since it follows a cleaved signal peptide, which inserts into the membrane as an SA sequence (Figure 2).

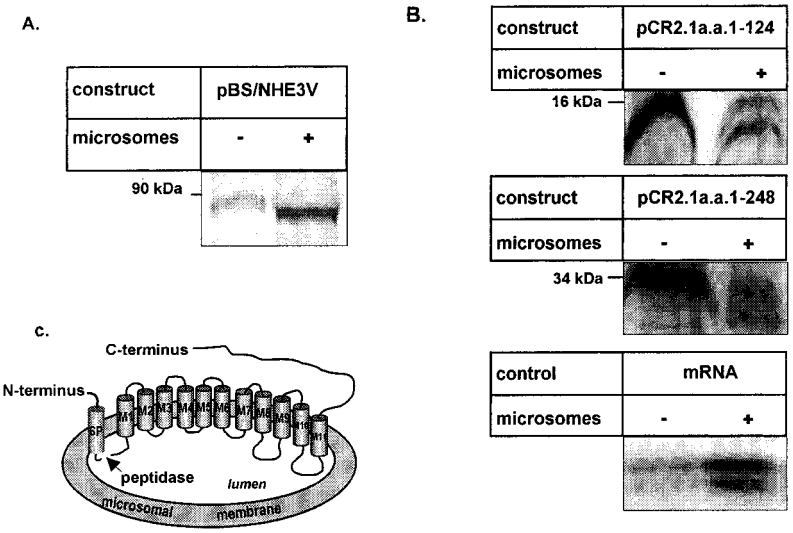

FIGURE 4: In vitro transcription/translation of the full-length NHE3 protein and a.a. 1−124 and 1−284. (A) Autoradiogram obtained by in vitro transcription/translation of full-length NHE3, cloned in the pBS expression vector, in the absence (−) and presence (+) of microsomes followed by SDS−PAGE to separate [^{35}S]Met-labeled translation products (lanes 1 and 2). (B) Similar studies are shown for NHE3 a.a. 1−124 (top) and a.a. 1−284 (bottom) cloned in the pCR2.1 expression vector. mRNA from kit was used as a positive control for microsome efficiency. (C) Scheme of the microsomal cotranslational processing of NHE3. Microsomal peptidases cause cotranslational signal peptide cleavage, which is followed by the shift down in molecular weight of NHE3. SP stands for signal peptide.

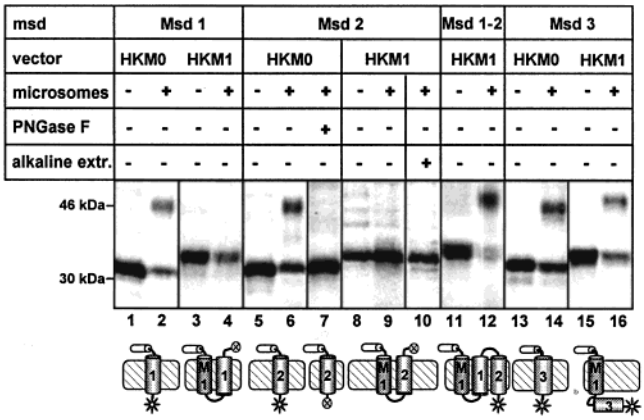

FIGURE 5: In vitro transcription/translation of the HKM0 and HKM1 vectors with insertions corresponding to putative msds 1, 2, and 3, combinations of msds 1 + 2, and the effect of PNGase F digestion and alkaline extraction of the fusion protein translated in the presence of microsomes. Autoradiograms of the [^{35}S]Met-labeled fusion proteins were obtained by in vitro transcription/translation of the HKM0 and HKM1 constructs in the absence (−) and presence (+) of microsomes followed by SDS−PAGE. HKM0/msd 2 construct translated in the presence of microsomes was incubated with PNGase F. The deglycosylated product was the same size as a product translated in the absence of microsome (lane 7). Lane 10 represents alkaline extraction of microsomal membranes after translation of HKM1/msd 2 in the presence of microsomes.

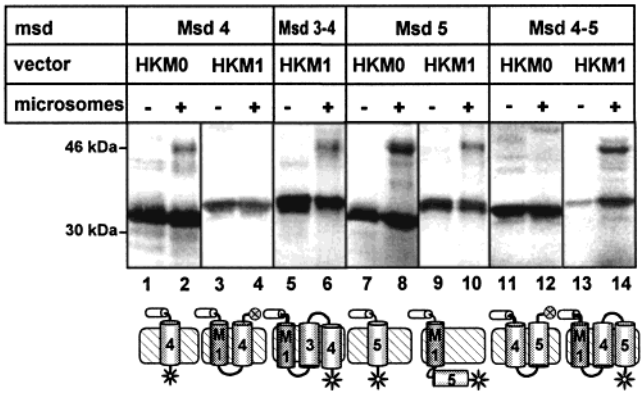

FIGURE 6: In vitro transcription/translation of the HKM0 and HKM1 vectors with insertions corresponding to putative msds 4 and 5 and combination of msds 3 + 4 and 4 + 5. Fusion proteins obtained by in vitro transcription/translation of cDNA in the presence of [^{32}S]Met were performed in the absence (−) and presence (+) of microsomal membranes. Reactions were followed by SDS−PAGE to separate the translated products, which were visualized by autoradiography.

Msd 3 (a.a. 110−133). Insertion of putative msd 3 into the HKM0 vector resulted in glycosylation of the translated protein in the presence of microsomes (Figure 5, lanes 13 and 14). The presence of the same sequence in the HKM1 vector did not prevent the translated fusion protein from being glycosylated in the presence of microsomes (Figure 5, lanes 15 and 16). The glycosylated band in lane 16 disappeared with deglycosylation (data not shown). These data suggested that putative msd 3 has the ability to act as an SA sequence, but lacks or has weak ST properties when inserted alone in HKM1. In the proposed NHE3 model (Figure 2) putative msd 3 was predicted to have an ST orientation in the membrane.

Msd 4 (a.a. 138−165). Insertion of putative msd 4 into the HKM0 vector resulted in glycosylation of the translated product in the presence of microsomes, while its presence in HKM1 prevented glycosylation of the translated product in the presence of microsomes (Figure 6, lanes 1−4). Therefore, putative msd 4 acts as both SA and ST sequences.

Msd 3−4 (a.a. 110−165). The construct msd 3−4 was used to determine whether C-terminal extension of putative msd 3 provides this sequence with ST activity. Insertion of putative msds 3−4 into the HKM1 vector resulted in glycosylation of the translated product in the presence of microsomes (Figure 6, lanes 5 and 6). This glycosylated band disappeared with deglycosylation (data not shown). Since msd 4 can act as both an SA and an ST, this suggested that this sequence contains a pair of transmembrane segments in which putative msd 4 acts as an SA and putative msd 3 acts as an ST sequence. Thus, when extended C-terminally,

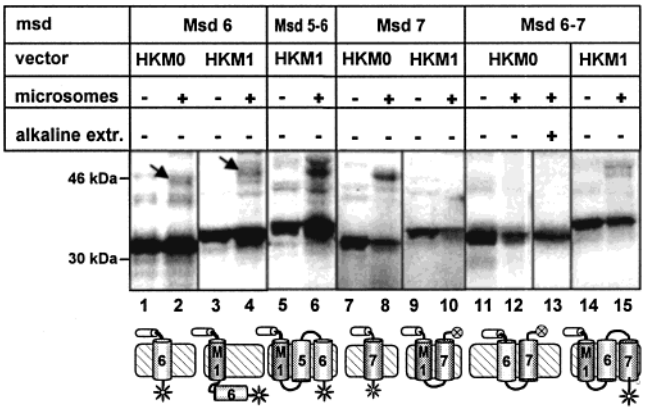

FIGURE 7: In vitro transcription/translation of the HKM0 and HKM1 vectors with insertions corresponding to putative msds 6 and 7 and combination of msd 5 + 6 and 6 + 7. Figure shows SDS−PAGE separated [^{35}S]Met-labeled fusion proteins, obtained by in vitro transcription/translation in the absence (−) and presence (+) of microsomal membrane, that were visualized by autoradiography. Arrows in lanes 2 and 4 indicate glycosylated products.

putative msd 3 has the ability to act as a ST sequence, which corresponds to its position in the NHE3 model in Figure 2.

Msd 5 (a.a. 174−199). The presence of putative msd 5 in the HKM0 and HKM1 vectors resulted in glycosylation of the translated product in the presence of microsomes (Figure 6, lanes 7−10). The glycosylated band in lanes 8 and 10 disappeared with deglycosylation (data not shown). Similar to msd 3, comparison with Figure 3, lane 4 indicates that the msd 5 has weak ST properties. Thus, putative msd 5 has the ability to act as an SA but lacks or has weak ST sequence when inserted alone into the expression vectors. In the proposed NHE3 model in Figure 2, putative msd 5 was predicted to act as an ST sequence.

Msd 4−5 (a.a. 138−199). Insertion of putative msd 4−5 into the HKM0 vector resulted in the absence of glycosylation of the translated product in the presence of microsomes (Figure 6, lanes 11 and 12). Recovery of this translation product after alkaline extraction verified its insertion into microsomal membranes (data not shown). These data suggested the presence of a pair of transmembrane segments, in which putative msd 4 acts as an SA and putative msd 5 acts as an ST sequence. Putative msd 5 thus has the ability to act as an ST when extended N-terminally. When putative msds 4−5 was inserted into the HKM1 vector, a glycosylated translation product was obtained in the presence of microsomes (Figure 6, lanes 13 and 14), demonstrating the presence of a pair of msds within this sequence.

Msd 6 (a.a. 207−230). Insertion of putative msd 6 into the HKM0 vector promoted weak glycosylation of the translated product in the presence of microsomes (Figure 7, lanes 1 and 2). The weak SA activity of putative msd 6 did not disappear after alkaline extraction (data not shown), confirming the membrane insertion of this sequence. There was a weak glycosylation when msd 6 was inserted into the HKM1 vector (Figure 7, lanes 3 and 4). The glycosylated band in lane 4 disappeared with deglycosylation (data not shown). Thus, these data indicate msd 6 as a weak SA and ST sequence, since the translated protein did not have the ability to completely prevent glycosylation in the HKM1 vector. The relatively low hydrophobic profile, according to the algorithm of Kyte and Doolittle (Figure 1) (*20*), was the most likely cause of the weak SA activity of putative msd 6. Msd 6 acts as an SA sequence in the NHE3 model in Figure 2.

Msd 5−6 (a.a. 174−230). When msd 5−6 was inserted into the HKM0 vector, no glycosylation of the translated product was obtained in the presence of microsomes (data not shown), suggesting the presence of a pair of msds in which putative msd 5 acts as an SA and msd 6 acts as an ST sequence. This ability of putative msd 6 to act as an ST sequence with N-terminal extension was used to test whether C-terminal extension provides putative msd 5 with ST activity when inserted in the HKM1 vector. As shown in Figure 7, lanes 5 and 6, translation of putative msd 5−6 inserted into the HKM1 vector resulted in glycosylation of the translated product in the presence of microsomes, which was PNGase F-sensitive (data not shown). Since N-terminally extended msd 6 can act as an SA or an ST, this demonstrates that C-terminal extension of putative msd 5 enables it to act as an ST sequence, as is predicted by its position in the NHE3 model (Figure 2).

Msd 7 (a.a. 248−276). The presence of putative msd 7 in the HKM0 vector promoted glycosylation of the translated product in the presence of microsomes and completely prevented glycosylation when expressed in the HKM1 vector (Figure 7, lanes 7−10). Therefore, putative msd 7 was able to act as both an efficient SA and an ST sequence.

Msd 6−7 (a.a. 207−276). The ability of putative msd 7 to act either as an SA or an ST sequence was used to examine whether C-terminal extension of putative msd 6 provides this sequence with ST activity. Insertion of putative msds 6−7 into the HKM1 vector resulted in glycosylation of the translated product in the presence of microsomes (Figure 7, lanes 14 and 15), which disappeared with deglycosylation (data not shown). This suggested the presence of a pair of transmembrane segments within this sequence in which putative msd 7 acts as an SA and putative msd 6 acts as an ST sequence. Thus, putative msd 6 has the ability to act as an ST sequence when extended C-terminally. When the same sequence was present in the HKM0 vector, a nonglycosylated translated product was obtained in the presence of microsomes (Figure 7, lanes 11 and 12), which was inserted into microsomal membranes as demonstrated by alkaline extraction (Figure 7, lane 13). These data confirmed the presence of a pair of msds in HKM0 in which putative msd 7 acts as an ST and putative msd 6 acts as an SA sequence as is predicted by their position in the NHE3 model in Figure 2.

Msd 8 (a.a 288−312). Translation of putative msd 8 in the HKM0 vector resulted in glycosylation of the translated product in the presence of microsomes (Figure 8, lanes 1 and 2). However, the presence of the same sequence in HKM1 did not prevent the translated product from being glycosylated in the presence of microsomes (Figure 8, lanes 3 and 4). This band disappeared with deglycosylation (data not shown). These data thus demonstrate that putative msd 8 acts as an SA sequence, which corresponds to its position in the proposed NHE3 model in Figure 2, but lacks the ability to act as an ST sequence when inserted alone in HKM1.

Msd 9 (a.a. 339−365). The presence of putative msd 9 in both the HKM0 and the HKM1 vectors resulted in glycosylation of the translated product when translated in the presence of microsomes (Figure 8, lanes 5−8). Thus, putative

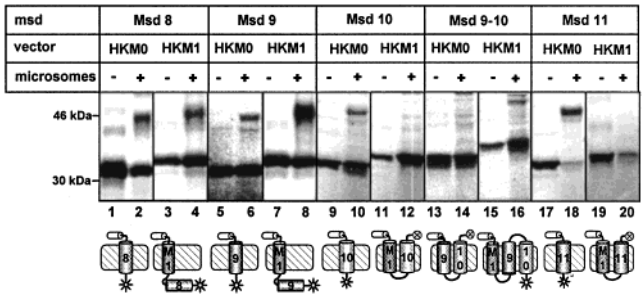

FIGURE 8: In vitro transcription/translation of the HKM0 and HKM1 vectors with insertions corresponding putative msds 8, 9, 10, and 11 and combinations of 9 and 10 including intervening amino acids. SDS−PAGE separated [^{35}S]Met-labeled fusion proteins obtained by in vitro transcription/translation in the absence (−) and presence (+) of microsomal membrane were visualized by autoradiography.

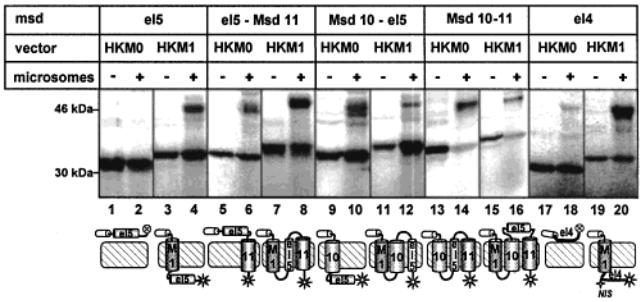

FIGURE 9: In vitro transcription/translation of the HKM0 and HKM1 vectors with insertions corresponding to the putative fifth extracellular loop (el5), putative fourth extracellular loop (el4), and combinations of putative el5−msd 11, msd 10−el5, and msds 10−11, including intervening amino acids. SDS−PAGE separated [^{35}S]-Met-labeled fusion proteins obtained by in vitro transcription/translation in the absence (−) and presence (+) of microsomal membrane were visualized by autoradiography.

msd 9 has the ability to act as an SA but not as an ST sequence when tested alone in the expression vectors.

Msd 10 (a.a. 369−395). Putative msd 10 acted as both SA and ST sequences. The sequence promoted glycosylation of translated product when inserted in the HKM0 vector and prevented glycosylation in the presence of microsomes when inserted in the HKM1 vector (Figure 8, lanes 9−12).

Msd 9−10 (a.a. 339−395). Since putative msd 9 was predicted to have ST activity in the proposed NHE3 model in Figure 2, C-terminal extension to include putative msd 10 was done to examine whether this extension provides putative msd 9 ST activity. The ability of putative msd 10 to act as both SA and ST sequences was used to test the membrane insertion properties of putative msd 9. Insertion of putative msd 9−10 into the HKM1 vector resulted in glycosylation of the translated product in the presence of microsomes (Figure 8, lanes 15 and 16). This band disappeared with deglycosylation (data not shown). This suggested the presence of a pair of transmembrane segments in the inserted sequence, in which putative msd 9 could insert into the membrane only in the ST direction because of the SA properties of putative msd 10 in this construct. The absence of glycosylation when putative msd 9−10 was present in the HKM0 vector confirmed the presence of a pair of transmembrane segments in this sequence (Figure 8, lanes 13 and 14). Thus, putative msd 9 has the ability to act as an ST sequence when extended C-terminally.

Msd 11 (a.a. 435−456). Msd 11 inserted in the HKM0 vector promoted glycosylation of the translated product suggesting SA properties. Translation of the same sequence in the HKM1 vector prevented glycosylation, demonstrating that this segment also acts as an efficient ST sequence (Figure 8, lanes 17−20).

As shown in Table 1, the highly hydrophobic region between putative msd 10 and 11, called extracellular loop 5 (el5) in Figure 2, was predicted to contain a transmembrane segment by five of seven algorithms. To examine the membrane properties of this region, a series of constructs containing this region alone or in combination with adjacent sequences was designed and tested.

El5 (a.a. 406−431). Translation of putative el5, inserted in the HKM0 vector did not promote glycosylation of the reporter sequence in the presence of microsomes, while its insertion in the HKM1 vector did not prevent glycosylation of the translated product (Figure 9, lanes 1−4). Thus, putative el5 does not have the ability to act either as an SA or an ST sequence when inserted alone into the HKM0 and HKM1 vectors. Given the increase in the nonglycosylated band in lane 4 as compared to Figure 3, lane 4, el5 may have weak ST properties.

El5−Msd 11 (a.a. 406−456). The effect of C-terminal extension on the membrane insertion properties of putative el5 was examined by using the ability of putative msd 11 to act as both SA and ST sequences (Figure 8, lanes 17−20). When the sequence el5−msd 11 was inserted into the HKM0 and HKM1 vectors, glycosylated translation products were obtained in the presence of microsomes (Figure 9, lanes 5−8). Given the established ability of msd 11 to act as an SA, the presence of the glycosylated product suggested that el5 has the ability to act as an ST but lacks the ability to act as an SA sequence when extended C-terminally.

Msd 10−El5 (a.a. 369−431). The ability of putative msd 10 to act as both SA and ST sequences was used to examine the effect of N-terminal extension on membrane insertion properties of putative el5. Insertion of the sequence msd 10−el5 in the HKM0 and HKM1 vectors resulted in glycosylation of the translated products in the presence of microsomes (Figure 9, lanes 9−12). The glycosylated band in lane 12 disappeared with deglycosylation (data not shown). This demonstrates that when putative el5 is extended N-terminally, el5 has the ability to act as an SA sequence but lacks the ability to act as an ST sequence.

Msd 10−11 (a.a. 369−456). To test membrane insertion capacities of putative el5 in combination with both N- and C-terminal extensions, the sequence containing putative msd 10 to msd 11 was inserted in both HKM0 and HKM1 vectors. The presence of putative msd 10−11 in the HKM0 vector resulted in glycosylation of the translated product in the presence of microsomes (Figure 9, lanes 13 and 14). Since the ability of putative msds 10 and 11 to act as both SA and ST sequence had been established (see Figure 8), the presence of the glycosylated translation product in the HKM0 construct suggested the presence of three transmembrane segments, 10 and 11 acting as an SA and el5 acting as an ST. When msd 10−11 was inserted in HKM1, a glycosylated translation product was obtained in the presence of microsomes (Figure 9, lanes 15 and 16). Glycosylation of the reporter sequence in this construct suggests the presence of

a pair of transmembrane segments within the inserted sequence, with putative msd 10 inserting in the membrane as an ST and msd 11 inserting as an SA sequence while putative el5 remains outside of the membrane. Taken together, these data suggest that putative el5 does not have the ability to act as an msd when tested alone, while some of its combinations with adjacent putative msds suggests that this sequence has some membrane insertion properties that directly depend on the adjacent sequences.

El4 (a.a. 320−339). Recent studies on NHE1 using an enzymatic cleavage approach showed that the last two putative extracellular loops are not exposed to the extracellular medium (*25*). These two loops correspond to putative el4 and el5 in Figure 2. Since they acted in a similar manner, we tested putative el4 to determine whether it has membrane-spanning capacity even though it was not predicted to be an msd by any algorithm in Table 1. Insertion of the sequence Lys^{320}−Lys^{339}, containing almost the entire putative el4, into the HKM0 vector did not promote glycosylation of the reporter sequence in the presence of microsomes (Figure 9, lanes 17 and 18). Translation of the same sequence in the HKM1 vector did not prevent glycosylation of the translated product. However, the molecular size shift of the glycosylated band was ∼15 kDa, which suggested that six potential core glycosylation sites were glycosylated in the translated product (Figure 9, lanes 19 and 20). This shift in size is consistent with glycosylation of both the reporter sequence of HKM1 and the single N-glycosylation consensus site present in putative el4. These data suggest that putative el4 does not have the ability to act either as an SA or an ST sequence and that the native single N-glycosylation consensus site of putative el4 was exposed to the lumen of microsomes when putative el4 was present in the HKM1 vector.

DISCUSSION

The data presented in this paper provide new insights into NHE topology by demonstrating that NHE3 contains a cleavable N-terminal signal sequence followed by 11 putative msds. To date, studies of NHE3 structure and function have been based on a NHE3 topology model of 12 msds and N- and C-termini, both on the intracellular side of the membrane, derived mostly from hydropathy analysis. However, there is still little biochemical evidence to support this NHE3 topology model. Therefore, the aim of this study was to systematically test the membrane insertion properties of each predicted putative msd of NHE3. An in vitro transcription/translation approach was used, which has already been successfully used to test the membrane topology of several integral membrane proteins including H,K-ATPase (*26*), Ca-ATPase (*28*), CCK-A receptor (*17*), P-type ATPase from *Helicobacter pylori* (*29*), and the intestinal Na^+-bile acid cotransporter (*30*). The in vitro transcription/translation method is based on the ability of membrane proteins to integrate cotranslationally into the endoplasmic reticulum membrane during protein synthesis. This integration in the membrane is regulated by a sequential SA/ST mechanism in which consecutive hydrophobic segments insert into the membrane with alternating orientation.

In vitro transcription/translation analysis is limited in determining the actual membrane orientation of putative msds, due to the ability of most hydrophobic msds to insert into the membrane in both SA and ST directions. Therefore, the actual orientation of putative msds of NHE3 in the membrane was deduced from the membrane location of the N- and C-termini of NHE3 plus the total number of msds identified. Recent studies, based on the ability of antibodies to bind inserted epitopes without cell permeabilization, suggested that regions containing residues Gln^{38} and Ile^{38}−Gly^{40} in NHE1 and NHE3, respectively, face the extracellular side of the membrane (*10*, *15*, *25*). Furthermore, NHE1 was shown to be N- and O-glycosylated on the first extracellular loop (*13*). Taken together, these data suggested that the first loop of NHE3 is located extracellularly. Studies in which an epitope tag fused to the NHE1 extreme N-terminus was not recognized by antibodies after cell permeabilization (*12*) suggested that the NHE N-terminus might be cleaved cotranslationally as part of a signal sequence. The SignalP algorithm (*27*) supported this speculation for NHE3 by predicting the presence of a signal peptide cleavage site between Gly^{29} and Ala^{30}. Results in the current study demonstrate, by using the ability of the signal peptidases present in the lumen of microsomes to cleave the signal peptide during protein processing, that NHE3 contains a cleavable signal peptide. This cleavable signal peptide is probably responsible for targeting NHE3 to the microsomal membrane and for the initial SA insertion process that translocates the following sequence of NHE3 into the lumen of microsomes. During NHE3 processing, the signal peptide appears to be cleaved off and the NHE3 N-terminus remains on the extracellular side of the membrane. The current studies should not be generalized to all NHEs, since the NHEs vary greatly in this part of the molecule.

Taken together, evidence for an extracellular N-terminus and an intracellular C-terminus (see the introduction) is indicative of an odd number of transmembrane segments in NHE3. This is supported by the fact that the transcription/translation technique identified 11 putative msds following the signal peptide. Hence, using the presence of a cleavable signal peptide in NHE3 as a starting point in defining the actual membrane orientation of transmembrane segments, in the proposed NHE3 model in Figure 2 putative msds 1, 3, 5, 7, 9, and 11 are predicted to act as ST, while putative msds 2, 4, 6, 8, and 10 are predicted to act as SA sequences.

On the basis of the experimental results obtained, putative msds of NHE3 can be separated into three groups. Group I includes six putative msds (msds 1, 2, 4, 7, 10, and 11) that demonstrated both SA and ST activity when tested alone in the expression vectors. Group II includes five putative msds (msds 3, 5, 6, 8, and 9) that were able to act only as a SA sequence when tested alone in the expression vectors. The extension of putative msds 3, 5, 6, and 9 to include the immediately C-terminal putative msd provided each of these putative msds with ST activity. In analysis of these pairs of msds, we used the ability of the second putative msd to insert into the membrane in either of two directions (SA/ST). In this approach, the actual orientation of the second putative msd in the constructs depended on the insertion properties of the preceding putative msd in the pair. Interestingly, some of these putative msds also had the ability to act as ST sequences after being extended N-terminally. These data thus suggest that membrane insertion and orientation of putative msds of NHE3 is a process controlled by cooperative action of sequential putative msds, not simply by the presence of

hydrophobic domains inserting with alternating orientation. In addition, the cooperative action of adjacent putative msds also has the ability to increase insertion efficiency of putative msds with a low hydrophobic profile. N-terminal extension of the low hydrophobic putative msd 6 of NHE3 significantly increased its efficiency in acting as an SA sequence (Figure 7, lanes 5 and 6). These data support the recent notion that domains with very low hydrophobic profiles are able to act as an msd when translated as a part of the native sequence of the protein despite their inability to act as an msd when tested alone (*31*). Another possibility for these results is that the boundaries of some putative msds of NHE3 might not be predicted accurately despite considering seven algorithms and extending the sequences to allow inclusion of the entire msd.

In group III, we included the region placed in putative extracellular loop 5 (el5), which was predicted by the hydropathy profile to contain a transmembrane segment, but the presence of an msd could not be confirmed by assessing membrane-insertion properties of putative el5 inserted alone in the HKM0/HKM1 vectors. This sequence showed inconsistent membrane insertion properties when extended to include the immediate C- and/or N-terminal putative msd. Thus, these data suggest that putative el5 associates with the membrane in a way that could not be adequately defined by this in vitro transcription/translation technique.

Recent studies showed that the last two extracellular loops of NHE1 are not exposed to extracellular medium. It was suggested that these loops might lie along the membrane surface or be folded within the protein (*25*). Though putative el4 of NHE3 does not act as an msd by itself, preliminary results showed that this region is able to associate with the membrane when extended N-terminally (data not shown). In addition, glycosylation in these transcription/translation studies of a single N-glycosylation consensus sequence (a.a. 325−327) present within putative el4 (Figure 9, lanes 19 and 20), which is not glycosylated in the native protein, further supports an association of this part of NHE3 when it is in the native protein in a way that inhibits microsomal access to this sequence. Of note, this sequence is preserved in NHE1−3 but it is not glycosylated in any of these NHEs (*13*, *14*).

On the basis of the constraint that NHE3 has an odd number of msds, we suggest two alternative topological models. In the first, shown in Figure 2, putative el4 faces the extracellular side of the membrane, while putative el5 associates with the membrane to form a P-loop in the membrane. Since such P-loops appear to be involved in forming the ion-transporting domain or the selective filter in other transport proteins (*32*), we suggest that extracellular loop 5 may be involved in forming the Na^+- and H^+-transporting domain and might interact with the most highly conserved part of the NHEs (msds 5/6) and with the sites shown to be involved in amiloride sensitivity (msds 3 and 8). In the second model, putative el5 and el4 both act as msds. Therefore, this model of NHE3 has 13 msds. In preliminary studies, el4 also had some membrane insertion properties, although results were somewhat contradictory similar to the studies with el5. Different approaches than the transcription/translation-based topology studies described here will be required to determine whether el4 and el5 are msds; however, given that el4 was not predicted to be an msd by any of the algorithms, we favor the 11 msd model.

After this manuscript was submitted, a study of the topology of NHE1 using a different approach, substituted cysteine accessibility analysis, was reported (*33*). Assignment of the first part of the exchanger (TM1 to TM8) was similar to our model, except that (1) there was no evidence for the existence of a cleavable signal peptide, (2) the area between our msds 8 and 11. Both models have 2 msds and a "P loop" in this area. However, the "P loops" are in different locations. Wakabayashi et al. concluded that extracellular loop 5 (terminology as in Figure 2) is an msd as well as supplying an intracellular and extracellular loop, while msd 9 may form a P-loop. This result for NHE1 supports the observation that el5 is a critical functional domain. However, these differences suggest that study of topology of these areas will have to be done by still other techniques to allow determination of whether these differences are due to differences in NHE isoforms or in the techniques used to define membrane topology.

In summary, in vitro transcription/translation studies have provided new insights into NHE topology by demonstrating that NHE3 (i) contains a cleavable signal peptide, (ii) has 11 (or less likely 13) rather than 12 transmembrane segments that insert into the membrane with alternating orientation, and (iii) has an extracellular loop 5 that appears to associate with the membrane in a P-loop-like structure.

REFERENCES

1. Wakabayashi, S., Shigekawa, M., and Pouyssegur, J. (1997) *Physiol. Rev. 77*, 51−74.
2. Wakabayashi, S., Ikeda, T., Noel, J., Schmitt, B., Orlowski, J., Pouyssegur, J., and Shigekawa, M. (1995) *J. Biol. Chem. 270*, 26460−26465.
3. Levine, S. A., Montrose, M. H., Tse, C. M., and Donowitz, M. (1993) *J. Biol. Chem. 268*, 25527−25535.
4. Yun, C. H., Tse, C. M., and Donowitz, M. (1995) *Proc. Natl. Acad. Sci. U.S.A. 92*, 10723−10727.
5. Hoogerwerf, W. A., Tsao, S. C., Devuyst, O., Levine, S. A., Yun, C. H., Yip, J. W., Cohen, M. E., Wilson, P. D., Lazenby, A. J., Tse, C. M., and Donowitz, M. (1996) *Am. J. Physiol. 270*, G29−41.
6. Sardet, C., Counillon, L., Franchi, A., and Pouyssegur, J. (1990) *Science 247*, 723−726.
7. Levine, S. A., Nath, S. K., Yun, C. H., Yip, J. W., Montrose, M., Donowitz, M., and Tse, C. M. (1995) *J. Biol. Chem. 270*, 13716−13725.
8. Bertrand, B., Wakabayashi, S., Ikeda, T., Pouyssegur, J., and Shigekawa, M. (1994) *J. Biol. Chem. 269*, 13703−13709.
9. Nath, S. K., Kambadur, R., Yun, C. H., Donowitz, M., and Tse, C. M. (1999) *Am. J. Physiol. 276*, C873−882.
10. Donowitz, M., Kambadur, R., Zizak, M., Nath, S., Akhter, S., and Tse, M. (1997) *Gastroenterology 112*, A360.
11. Biemesderfer, D., DeGray, B., and Aronson, P. S. (1998) *J. Biol. Chem. 273*, 12391−12396.
12. Wakabayashi, S., Fafournoux, P., Sardet, C., and Pouyssegur, J. (1992) *Proc. Natl. Acad. Sci. U.S.A. 89*, 2424−2428.
13. Counillon, L., Pouyssegur, J., and Reithmeier, R. A. (1994) *Biochemistry 33*, 10463−10469.
14. Tse, C. M., Levine, S. A., Yun, C. H., Khurana, S., and Donowitz, M. (1994) *Biochemistry 33*, 12954−12961.
15. Kurashima, K., Szabo, E. Z., Lukacs, G., Orlowski, J., and Grinstein, S. (1998) *J. Biol. Chem. 273*, 20828−20836.
16. Bamberg, K., and Sachs, G. (1994) *J. Biol. Chem. 269*, 16909−16919.
17. Bayle, D., Weeks, D., and Sachs, G. (1997) *J. Biol. Chem. 272*, 19697−19707.

18. Rao, M. J. K., and Argos, P. (1986) *Biochim. Biophys. Acta 869*, 197−214.
19. Rost, B., Casadio, R., Fariselli, P., and Sander, C. (1995) *Protein Sci. 4*, 521−533.
20. Kyte, J., and Doolittle, R. F. (1982) *J. Mol. Biol. 157*, 105−132.
21. Eisenberg, D., Schwarz, E., Komaromy, M., and Wall, R. (1984) *J. Mol. Biol. 179*, 125−142.
22. Jones, D. T., Taylor, W. R., and Thornton, J. M. (1994) *Biochemistry 33*, 3038−3049. (http://globin.bio.warwick.ac.uk/~jones/memsat.html)
23. Rost, B., Fariselli, P., and Casadio, R. (1996) *Protein Sci. 5*, 1704−1718.
24. von Heijne, G. (1992) *J. Mol. Biol. 225*, 487−494.
25. Shrode, L. D., Gan, B. S., D'Souza, S. J., Orlowski, J., and Grinstein, S. (1998) *Am. J. Physiol. 275*, C431−439.
26. Bamberg, K., and Sachs, G. (1994) *J. Biol. Chem. 269*, 16909−16919.
27. Nielsen, H., Engelbrecht, J., Brunak, S., and von Heijne, G. (1997) *Protein Eng. 10*, 1−6. (http://www.cbs.dtu.dk/services/SignalP/)
28. Bayle, D., Weeks, D., and Sachs, G. (1995) *J. Biol. Chem. 270*, 25678−25684.
29. Melchers, K., Weitzenegger, T., Buhmann, A., Steinhilber, W., Sachs, G., and Schafer, K. P. (1996) *J. Biol. Chem. 271*, 446−457.
30. Hallen, S., Branden, M., Dawson, P. A., and Sachs, G. (1999) *Biochemistry 38*, 11379−11388.
31. van Geest, M., Nilsson, I., von Heijne, G., and Lolkema, J. S. (1999) *J. Biol. Chem. 274*, 2816−2823.
32. Tai, K. K., and Goldstein, S. A. (1998) *Nature 391*, 605−608.
33. Wakabayashi, S., Pang, T., Su, X., and Shigekawa, M. (2000) *J. Biol. Chem. 275*, 7942−7949.
34. Tusnady, G. E., and Simon, I. (1998) *J. Mol. Biol. 283*, 489−506.
35. http://ulrec3.unil.ch/software/TMPRED_form.html

BI000870T